

PAPER • OPEN ACCESS

## Electrical Resistivity of Wire Arc Sprayed Zn and Cu Coatings for In-Mold-Metal-Spraying

To cite this article: K Bobzin *et al* 2018 *IOP Conf. Ser.: Mater. Sci. Eng.* **373** 012011

View the [article online](#) for updates and enhancements.

### Related content

- [Part weight verification between simulation and experiment of plastic part in injection moulding process](#)  
M. A. M Amran, N. Idayu, K. M. Faizal et al.
- [Study on the fabrication and physical properties of cold-sprayed, Cu-based amorphous coating](#)  
K A Lee, D J Jung, D Y Park et al.
- [Superconductivity and Electrical Resistivity in the T-Phase  \$\text{Pr}\_{2-x}\text{La}\_x\text{Ce}\_y\text{CuO}\_4\$](#)   
Yoji Koike, Akihiro Kakimoto, Mitsunori Mochida et al.

# Electrical Resistivity of Wire Arc Sprayed Zn and Cu Coatings for In-Mold-Metal-Spraying

K Bobzin<sup>1</sup>, M Öte<sup>1</sup>, M A Knoch<sup>1</sup>, X Liao<sup>1,\*</sup>, Ch Hopmann<sup>2</sup> and P Ochotta<sup>2</sup>

<sup>1</sup> Surface Engineering Institute, RWTH Aachen University, Kackertstr. 15, 52072 Aachen, Germany

<sup>2</sup> Institute of Plastics Processing, RWTH Aachen University, Seffenter Weg 201, 52074 Aachen, Germany

\* e-mail: liao@iot.rwth-aachen.de

**Abstract.** Electrical functionalities can be integrated into plastic parts by integrating thermally sprayed metal coatings into the non-conductive base material. Thermally sprayed conducting tracks for power and signal transmission are one example. In this case, the electrical resistance or resistivity of the coatings should be investigated. Therefore, the electrical resistivity of wire arc sprayed Zn and Cu coatings has been investigated. In case of Zn coatings, spray distance, gas pressure and wire diameter could be identified as significant influencing parameters on the electrical resistivity. In contrast, process gas, gas pressure and voltage do have a significant influence on the electrical resistivity of Cu coatings. Through the use of the In-Mold-Metal-Spraying method (IMMS), thermal degradation can be avoided by transferring thermally sprayed coating from a mold insert onto the plastic part. Therefore, the influence of the transfer process on the electrical resistance of the coatings has also been investigated.

## 1. Introduction

Due to the various advantageous properties of plastics, e.g. low density and high chemical resistance, this type of materials has been widely used in different fields. Although these properties may be desired for certain cases, sometimes the opposite properties are required for certain applications. For example, plastics are usually good electrical insulators, which is disadvantageous for applications where the electrical conductivity is required, such as power and signal transmission. In this case, the concept of combining plastic and metal in a single part can be applied, in order to fulfill the requirement of the application and benefit from other properties of the plastics at the same time. There are different approaches for fabricating such hybrid parts, including the application of metal coatings onto the part surface by means of different coating technologies. Due to the high efficiency and the ability of processing different materials, thermal spraying has attracted lots of interest regarding coating deposition, including metal coatings, onto plastic parts.

The results in the literature show, on the one hand, the possibility of fabricating metal coatings on plastic substrates by means of thermal spraying. On the other hand, the thermal and kinetic energy of the particles and the process gas needs to be adjusted to avoid damage or extensive softening of the substrate [1-8]. This leads to difficulties for coating deposition on substrates made of widely used engineering plastics, which exhibit relatively lower thermal resistance in comparison to the more expensive high performance plastics. Therefore, a new approach, the In-Mold-Metal-Spraying



(IMMS), has been developed at Surface Engineering Institute (IOT) and Institute of Plastic Processing (IKV) of RWTH Aachen University. To avoid the direct contact between the plastic substrate and the high temperature particles and gas, the metal coatings are first applied onto the surface of the mold cavity or the mold insert for injection molding. By using a suitable pre-treatment of the surface, e.g. glass bead blasting, a relatively low bond strength of the coating to the mold cavity or the mold insert surface can be achieved. Therefore, the coating can be transferred to the plastic part after the injection molding process [9-12]. The hybrid metal/plastic parts fabricated by IMMS can be used in different applications, such as conducting tracks for signal and power transmission. To the knowledge of the authors, the requirement on the electrical resistance  $R$  or the electrical resistivity  $\rho_{el.}$  of such conducting tracks depends on the specific application, and there is no unique standard for all applications. Generally, a low electrical resistivity of the conducting track is desired, in order to ensure high signal quality. In the current study, the process parameters that might have significant influence on  $\rho_{el.}$  and their effects were identified and confirmed using two staged design of experiments (DoE) in case of Zn and Cu coatings.

## 2. Experimental setup

In the first stage of DoE, the process parameters of WAS that might have significant effect were identified using fractional factorial design of experiments. The effects of chosen parameters were further confirmed in the second stage of DoE using full factorial design of experiments. Furthermore, the influence of the transfer process on the coating was investigated by the comparison of the electrical resistance of transferred and detached coatings.

### 2.1. Experimental methods for the determination of the coating's electrical resistivity

In the current study, steel sheets made of 1.0037 (AISI 1015) have been used as mold inserts which are the carrier body for the coatings at the same time. The coated carrier bodies can be placed into the mold cavity for coating transfer. The coatings were deposited by means of WAS using the spraying unit OSU G30/4SF-Push-LD/U2 (Oerlikon Metco AG, Winterthur, Switzerland) with a closed, nonadjustable nozzle system. After blasting the carrier body with glass beads using a blasting unit Superbaby II (BHS, Aachen, Germany), five coatings in the shape of conducting tracks with defined width  $b$  and length  $l$  can be fabricated by using a mask per experiment run, see figure 1.

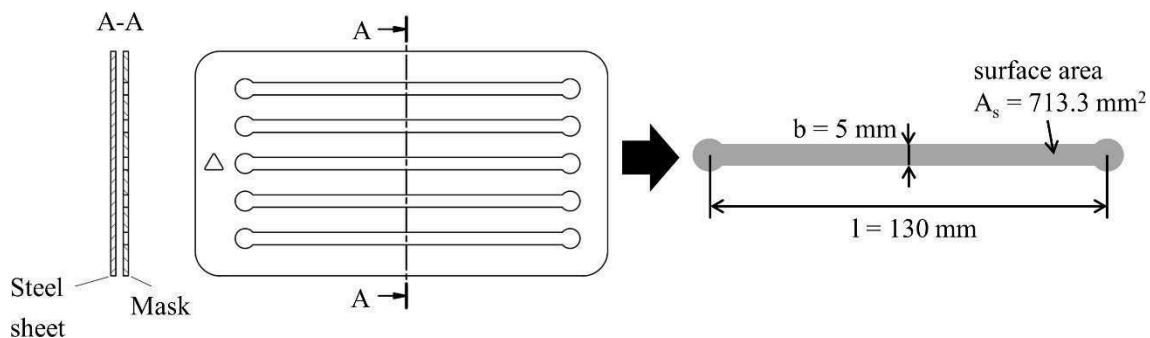


**Figure 1.** Fabrication of coatings in the shape of conducting tracks using a mask.

The influence of the process parameters of WAS on the coating's electrical resistivity was investigated in the first step of the current study. To avoid an overlap of the effects from WAS and injection molding, the deposited coatings were not transferred onto plastic parts, but were directly detached from the carrier bodies. The electrical resistance  $R$  is measured by means of 4-wire sensing using an ohmmeter ILOM-508A (RS components GmbH, Mörfelden-Walldorf, Germany), which is necessary to eliminate the influence of lead and contact resistance for a precise determination of small electrical resistance [13]. The electrical resistivity  $\rho_{el.}$  can be calculated as shown in equation 1 [14]:

$$\rho_{el.} = R \cdot \frac{A_c}{l} \quad (1)$$

The length  $l$  is defined by the mask. The cross-sectional area  $A_c$  can be determined by multiplication of the width  $b$  and the thickness  $t$  of the coating. Because wire arc sprayed coatings exhibit usually a rough surface and inhomogeneity in thickness, the conventional method of determining coating thickness by examining the cross sections of the coating requires great measurement effort to obtain a representative coating thickness. In the current study, two alternative methods were used to determine the cross-sectional area  $A_c$ . In the first stage of the DoE, the weight  $m$  of the coatings was measured. The volume  $V$  of the coating can be roughly estimated by dividing  $m$  by the density  $\rho$  of the feedstock material. Dividing  $V$  by the surface area of the coating  $A_s$ , which is shown in figure 1, yields the average thickness of the coating. Therefore, a rough estimation  $\rho_{el,w}$  of the coating's electrical resistivity is:

$$\rho_{el,w} = R \cdot \frac{m \cdot b}{\rho \cdot A_s \cdot l} \quad (2)$$

Although there is usually a difference between the densities of the feedstock material and the coating, this method enables an approximation of the coating's electrical resistivity. Furthermore,  $m$  can be measured more quickly and precisely. To avoid the influence of the density difference between the coating and the feedstock materials on the result,  $V$  can be directly determined by pycnometer measurement. However, the measurement duration with pycnometer is much longer than the weight measurement. Hence, this method has only been used in the second stage of the DoE experiment, after the amount of to be investigated parameters is reduced. In order to distinguish the electrical resistivity obtained by the two methods, the coating's resistivity estimated by the second method is referred to as  $\rho_{el,v}$  which is calculated by equation 3:

$$\rho_{el,v} = R \cdot \frac{V \cdot b}{A_s \cdot l} \quad (3)$$

## 2.2. The procedure of DoE

The feedstock materials, Zn and Cu, were investigated. For each material, a fractional factorial design of experiments with two levels for each process parameter was used for the first stage of DoE. Each experiment was carried out once. In case of Zn coatings, the process parameters indicated in Table 1 were investigated in the first stage. To ensure a stable process, the voltage can only be adjusted in a very small range for depositing Zn coatings with the used arc spraying unit. Therefore, the voltage  $U$  has not been included and was set at  $U = 22$  V. The two levels of the other parameters are labeled with “-” and “+” respectively, and their corresponding settings are listed in Table 1. The traverse velocity of the spray gun  $v$  was set at  $v = 200$  and  $450$  m/s for the feed rate  $F$  of  $F = 5.8$  and  $13.5$  kg/h, respectively, in order to achieve a similar coating thickness in all experiments. The spraying gun travels once across the carrier body surface to deposit the coatings in the experiments. To avoid the variation of the process condition caused by changing the wires, the experiments in the first stage were divided in two groups regarding the wire diameter, when the experiments were conducted. In each group, the wire diameter is kept constant, while the settings of the other parameters were varied randomly.

**Table 1.** Levels of the parameters in the screening experiment for Zn coating.

Parameter	-	+
<b>A (wire diameter)</b>	1.6 mm	2.5 mm
<b>B (gas)</b>	N <sub>2</sub>	Pressured air
<b>C (feed rate)</b>	5.8 kg/h	13.5 kg/h
<b>D (pressure)</b>	2.5 bar	4.5 bar
<b>E (stand-off distance)</b>	50 mm	150 mm

In case of Cu coatings, Cu wire with the diameter  $\varnothing$  of  $\varnothing = 2.5$  mm was not available in the current study. Furthermore, in the previous study N<sub>2</sub> instead of pressured air was used as atomizing gas

leading to a much lower electrical resistivity using the same spraying unit with a different nozzle system [15]. Therefore, the two parameters, the wire diameter  $\varnothing$  and the atomizing gas G, are excluded in the first stage of DoE for Cu coatings. They were set to  $\varnothing = 1.6$  mm and  $G = N_2$  respectively. The voltage can be adjusted in a greater range in case of depositing Cu coatings. Therefore, the voltage was included in the screening experiment. The parameters and their levels are listed in Table 2. The traverse velocity  $v$  of the spraying gun was set to  $v = 337.5$  and  $675$  m/s for the feed rate  $F$  of  $F = 4.8$  and  $10.5$  kg/h, respectively to achieve a similar coating thickness in all experiments. The spraying gun traveled two times across the carrier body surface to deposit the coatings in the experiments.

**Table 2.** Levels of the parameters in the screening experiment for Cu coating.

Parameter	-	+
<b>A (pressure)</b>	3 bar	6 bar
<b>B (stand-off distance)</b>	50 mm	100 mm
<b>C (voltage)</b>	31 V	40 V
<b>D (feed rate)</b>	4.8 kg/h	10.5 kg/h

After the first stage of DoE, the effect caused by changing a parameter from the low level to the high level was determined based on the obtained results. Two parameters were chosen for the second stage of DoE with full factorial design of experiments. The level of the parameter's effect determined in the screening experiment is not the sole criterion for choosing the parameters for the second stage of DoE. Other aspects, such as the possible influence on the transferability of the coating, should also be considered. The approach of the second stage of DoE for Zn and Cu coatings will be introduced in section 3 after that the results of the first stage are presented and discussed.

### 2.3. Investigation of the influence of the transfer process on the coating's electrical resistance

Besides the parameters of WAS processes, the coating's electrical properties might also be influenced by the transfer process. Because the coating adheres stronger to the plastic parts than to the carrier body, the detachment of the coatings from the plastic part without damaging them is difficult. The measurement of the coating's cross-sectional area or thickness with the assistance of pycnometer is no longer possible for transferred coatings. Therefore, the comparison of coating's electrical resistivity before and after transfer process is not a suitable method to evaluate the effect of the transfer process due to the different measurement methods for detached and transferred coatings. In the current study, the coating's electrical resistance instead of the electrical resistivity is used to determine the effect of the transfer process. Ten carrier bodies were coated for each material using the same WAS parameter. The coatings on five of them are transferred to plastic parts by means of IMMS using a polyamide 66 SCHULAMID 66 GF35 H4 with 35 vol. % of glass fibers (A. Schulman GmbH, Kerpen, Germany), while the coatings on the other five carrier bodies were directly detached for the measurement of the electrical resistance. The electrical resistance of the transferred coatings was also measured and compared to that of the detached coatings.

## 3. Results and discussion

The experiments have been conducted as described in section 2. Their results are presented and discussed in this section.

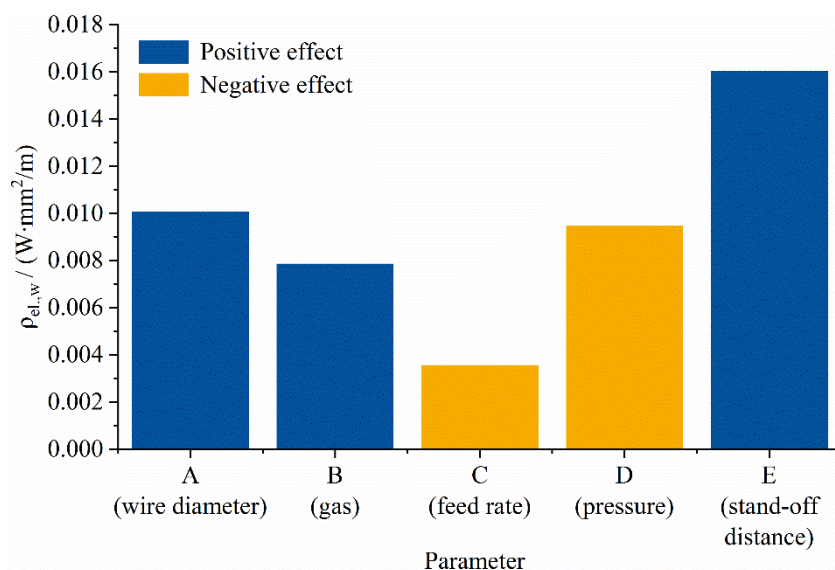
### 3.1. Influence of WAS process on the electrical resistivity of Zn coatings

A  $2^{5-1}$  fractional factorial design of experiments is constructed for Zn coatings as shown in Table 3. As mentioned above, the coating's electrical resistivity was obtained by measuring the weight of the coatings at this stage of DoE.

**Table 3.** The screening experiments in case of Zn coating.

No.	A (wire diameter)	B (gas)	C (feed rate)	D (pressure)	E (stand-off distance)	$\rho_{el,w}/$ ( $\Omega \cdot \text{mm}^2/\text{m}$ )
Zn-S-1	-	+	-	-	+	0.1194
Zn-S-2	+	+	-	-	-	0.1130
Zn-S-3	-	-	-	-	-	0.1056
Zn-S-4	+	-	-	-	+	0.1334
Zn-S-5	-	+	+	-	-	0.1095
Zn-S-6	+	+	+	-	+	0.1333
Zn-S-7	-	-	+	-	+	0.1111
Zn-S-8	+	-	+	-	-	0.1056
Zn-S-9	-	+	-	+	-	0.1047
Zn-S-10	+	+	-	+	+	0.1337
Zn-S-11	-	-	-	+	+	0.1013
Zn-S-12	+	-	-	+	-	0.0962
Zn-S-13	-	+	+	+	+	0.1089
Zn-S-14	+	+	+	+	-	0.1020
Zn-S-15	-	-	+	+	-	0.0924
Zn-S-16	+	-	+	+	+	0.1161

The effect of an investigated parameter can be calculated by subtracting the average  $\rho_{el,w}$  of the experiments with the parameter set at level “+” by the average  $\rho_{el,w}$  of the experiments with the parameter set at level “-”. The effects of the parameters on  $\rho_{el,w}$  are compared in figure 3. The stand-off distance has shown the highest effect and was chosen as one of the two parameters to be investigated in the second stage. The wire diameter and the pressure have shown similar effects. As mentioned above, the change of the wires might causes the variation of the process condition, so that the effects of other parameters would be overlapped. Therefore, the pressure was chosen as the second parameter for the full factorial design in the second stage. To confirm the effect of the wire diameter, a separate experiment series, which involves only the wire diameter, was also conducted.

**Figure 2.** Comparison of the effects of the parameters in the screening experiment for the Zn coating.

A  $2^2$  full factorial design of experiments has been conducted to investigate the effects of the parameters, stand-off distance and pressure, on the coating's electrical resistivity. It means that there are  $2^2$  different combinations of the settings of the two investigated parameters, (-, -), (+, -), (-, +) and (+, +). The experiments with one of these parameter combinations are referred as factorial points. One additional level labeled "0", which is the average of level "-" and "+", was used to define an additional experiment point, the center point, with the parameter combination (0, 0) in the experimental matrix. By this means, it can be examined if quadratic correlation between the coating's electrical resistivity and the two parameters exist. The levels of the two parameters are given in Table 4. Higher inlet pressure is possible, when  $N_2$  is used as atomizing gas. Furthermore, the results of the screening experiment show that higher gas pressure might be beneficial for achieving lower electrical resistivity. Therefore, the "-" and "+" levels of the pressure  $p$  were chosen as  $p = 3$  bar and 6 bar respectively. The settings of the other parameters, wire diameter  $\emptyset$ , gas  $G$ , feed rate  $F$ , voltage  $U$  and traverse velocity  $v$ , were chosen as  $\emptyset = 1.6$  mm,  $G = N_2$ ,  $F = 13.5$  kg/h,  $U = 22$  V and  $v = 450$  m/s, respectively.

**Table 4.** Levels of the stand-off distance and the pressure in the characterization experiment for Zn coating.

Parameter	-	0	+
<b>A (stand-off distance)</b>	50 mm	100 mm	150 mm
<b>B (pressure)</b>	3 bar	4.5 bar	6 bar

At this stage,  $\rho_{el,v}$  is measured and calculated as mentioned in section 2. The results are shown in Table 5. The experiments numbered Zn-C-1 to 4 in Table 5 are factorial points with two replications of each parameter combination. The center point, Zn-C-5, has been replicated four times. To confirm the significance of the effect of the wire diameter, a further parameter set, Zn-C-6, was used in addition to the factorial points and the center point. The feedstock material was Zn wires with the diameter  $\emptyset$  of  $\emptyset = 2.5$  mm in this parameter set. The settings of the other parameters of the center point, Zn-C-5, were also used for Zn-C-6.

**Table 5.** Results of the second stage of DoE for Zn coating.

No.	A (stand-off distance)	B (pressure)	Wire diameter /mm	$\rho_{el,v}/(\Omega\cdot\text{mm}^2/\text{m})$			
				Replication 1	Replication 2	Replication 3	Replication 4
<b>Zn-C-1</b>	-	-	1.6	0.0958	0.0976	-	-
<b>Zn-C-2</b>	-	+	1.6	0.0880	0.0884	-	-
<b>Zn-C-3</b>	+	-	1.6	0.1072	0.1098	-	-
<b>Zn-C-4</b>	+	+	1.6	0.1013	0.1006	-	-
<b>Zn-C-5</b>	0	0	1.6	0.0975	0.0992	0.0974	0.0991
<b>Zn-C-6</b>	0	0	2.5	0.1027	0.1020	0.1016	0.1018

In order to examine the significance of the effects of the parameters, the F-test has been applied on the results. The F-values, which are the ratio between the mean square caused by an effect and the mean square of the experimental error, of the two parameters and their interaction are determined. Due to the integration of a center point in the  $2^2$  design, the F-value of the quadratic effect can also be determined and used to examine the significance of a possible quadratic correlation. Details of the calculation of the F-value can be found in [16]. The F-values should be compared with a critical F-value, which corresponds to a chosen confidence level. In the current study, the confidence level is chosen as 95%. The results are shown in the Figure 4. The effects of the two investigated parameters are significant, and their interaction effect and the quadratic effect are insignificant.

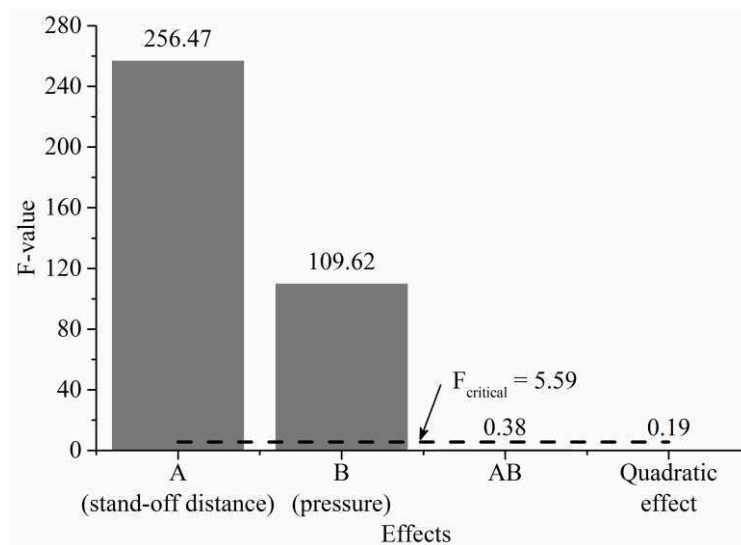


**Figure 3.** The F-values of the effects of stand-off distance and pressure, their interaction effect and the curvature compared with the critical F-value.

Based on the results, a linear model describing the correlation between  $\rho_{el,v}$  and the two parameters can be constructed. Since AB is insignificant, a model containing only A and B was constructed, see equation 4.

$$\rho_v / (\Omega \cdot \text{mm}^2 / \text{m}) = 0.0983 + 1.2775 \cdot 10^{-4} \cdot A / \text{mm} - 2.675 \cdot 10^{-3} \cdot B / \text{bar} \quad (4)$$

The correlation between  $\rho_{el,v}$  and the two parameters based on equation 4 is shown in the contour plot in figure 4. It shows that  $\rho_{el,v}$  decreases with decreasing stand-off distance and increasing pressure. The comparison of the coating’s electrical resistivity of the experiments Zn-C-5 and Zn-C-6 in figure 4b shows that the wire diameter exhibit an influence on the coating’s resistivity. However, the difference of the coating’s electrical resistivity caused by the different wire diameters is small.

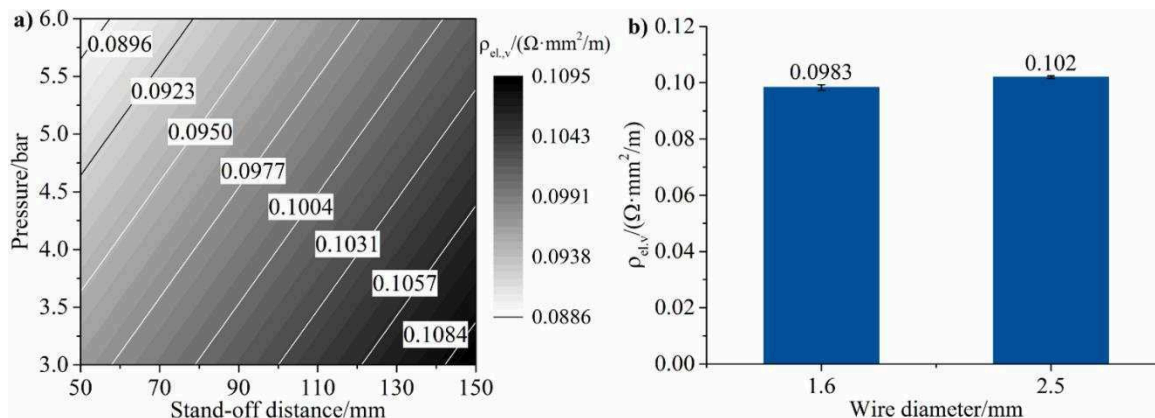


**Figure 4.** Contour plot of the correlation between  $\rho_{el,v}$ , the pressure and the voltage in case of Zn coating (a) and the effect of the wire diameter (b).

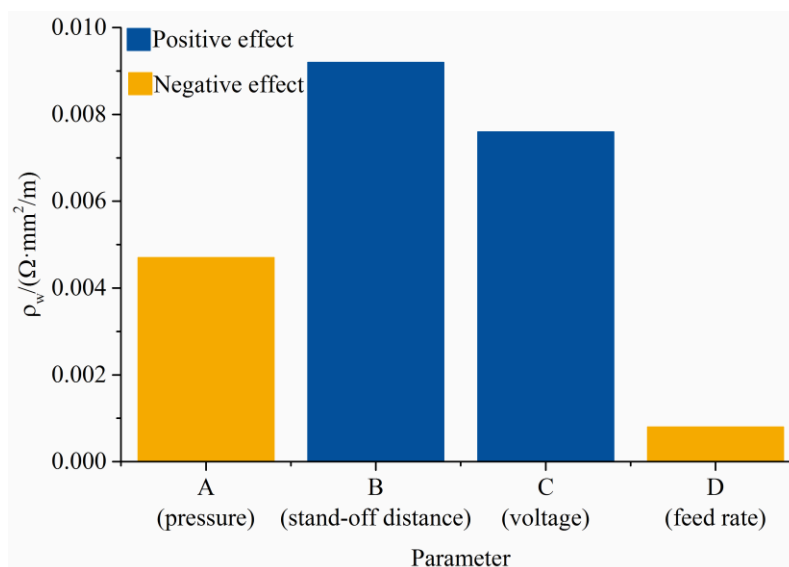
### 3.2. Influence of WAS process on the electrical resistivity of Cu coatings

The same procedure has been carried out for the investigation of Cu coatings as in case of Zn coatings. The parameter combinations of the  $2^{4-1}$  experiment matrix and the results are listed in Table 6.

**Table 6.** The screening experiments in case of Cu coating.

No.	A (pressure)	B (stand-off distance)	C (voltage)	D (feed rate)	$\rho_{el,w}$ /( $\Omega \cdot \text{mm}^2/\text{m}$ )
<b>Cu-S-1</b>	-	-	-	-	0.0348
<b>Cu-S-2</b>	+	-	-	+	0.0302
<b>Cu-S-3</b>	-	+	-	+	0.0416
<b>Cu-S-4</b>	+	+	-	-	0.0375
<b>Cu-S-5</b>	-	-	+	+	0.0398
<b>Cu-S-6</b>	+	-	+	-	0.0361
<b>Cu-S-7</b>	-	+	+	-	0.0525
<b>Cu-S-8</b>	+	+	+	+	0.0461

The effects of each parameter are calculated with the same procedure for Zn coatings described in section 3.1 and shown in figure 5. Although the stand-off distance has shown the highest effect among all parameters, the coating adhesion to the carrier body in the experiments with high stand-off distance is low. Lots of coatings detached already during the deposition process and were destroyed by the gas stream in the experiments with high stand-off distance. A higher coating adhesion to the carrier body can be achieved by using carrier bodies blasted with coarser glass beads. On the one hand, the use of the coarsest glass beads available in the current study with the size distribution of 200 to 300  $\mu\text{m}$  could not guarantee a sufficient adhesion. On the other hand, blasting with coarser blasting medium would result in a carrier body surface with more undercuts, which promotes the mechanical interlocking between the coating and the carrier body. This is disadvantageous for the coating transfer in IMMS, because the coating might be damaged at positions, where strong mechanical interlocking is present, during the transfer from the carrier body to the plastic part. Since this parameter would not be adjustable for the aimed application, the stand-off distance was not further investigated in the characterization experiment. The pressure and the voltage have been chosen instead as to be investigated parameters in the second stage. The feed rate has shown a negligible effect in comparison to the other three parameters.

**Figure 5.** Comparison of the effects of the parameters in the screening experiment for the Cu coating.

A  $2^2$  experiment design with center point was also used in the second stage of DoE for Cu coatings as in case of Zn coatings. The levels “-”, “+” and “0” of the pressure and the voltage are listed in Table 7. The level “0” of the voltage U should be  $U = 35.5$  V, which is the average of level “-” and “+”. Due to the stepwise adjustment of the voltage of the spraying unit with relays, the voltage cannot be set at exactly  $U = 35.5$  V. The closest possible value is  $U = 36$  V and was used as level “0” in the experiments. The settings of the other parameters, wire diameter  $\varnothing$ , gas G, feed rate F, the stand-off distance s and the traverse velocity v of the spraying gun, were chosen as  $\varnothing = 1.6$  mm,  $G = N_2$ ,  $F = 10.5$  kg/h,  $s = 50$  mm and  $v = 675$  m/s, respectively.

**Table 7.** Levels of the pressure and the voltage in the characterization experiment for Cu coating.

Parameter	-	0	+
<b>A (pressure)</b>	3 bar	4.5 bar	6 bar
<b>B (voltage)</b>	31 V	36 V	40 V

The parameter combinations of the experiments and the measured  $\rho_{el,v}$  were listed in Table 8. As in case of the Zn coatings, the experiments at the factorial points have been replicated twice, while the experiment at the center point has been replicated four times.

**Table 8.** Results of the second stage of DoE for Cu coatings.

No.	A (pressure)	B (voltage)	$\rho_{el,v}/(\Omega \cdot \text{mm}^2/\text{m})$			
			Replication 1	Replication 2	Replication 3	Replication 4
<b>Cu-C-1</b>	-	-	0.0347	0.0355	-	-
<b>Cu-C-2</b>	+	-	0.0292	0.0288	-	-
<b>Cu-C-3</b>	-	+	0.0490	0.0467	-	-
<b>Cu-C-4</b>	+	+	0.0348	0.0344	-	-
<b>Cu-C-5</b>	0	0	0.0359	0.0360	0.0358	0.0355

The F-values of the effects of the two parameters, their interaction effects and the quadratic effect were calculated and shown in figure 6. Both effects of the parameters and their interaction effect can be considered as significant based on the F-test. In contrast, the quadratic effect is not significant.

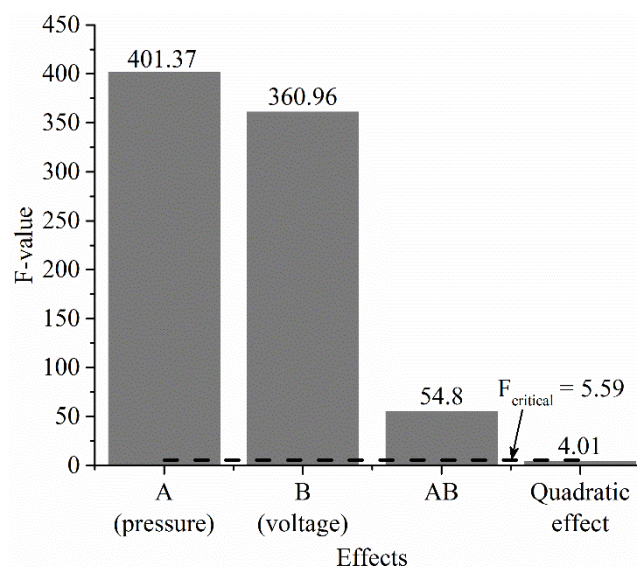


**Figure 6.** The F-values of the effects in the second stage of DoE for Cu coatings.

The correlation between the coating’s electrical resistivity and the parameters can be described by equation 5, which is derived by the experimental results shown in Table 8. Because the interaction effect of the two parameters has a F-value higher than  $F_{critical}$ , the term A·B is included in the equation.

$$\rho_{el,v}/(\Omega \cdot \text{mm}^2/\text{m}) = -0.0276 + 6.1759 \cdot 10^{-3} \cdot A/\text{bar} + 2.1111 \cdot 10^{-3} \cdot B/\text{V} - 2.6482 \cdot 10^{-3} \cdot A \cdot B/(\text{bar} \cdot \text{V}) \quad (5)$$

The contour plot based on equation 5 is shown in figure 7a. The coating’s electrical resistivity increases with decreasing pressure and increasing voltage. The contour lines are curved, which is caused by the interaction effect of the two parameters. The effect of the voltage is slightly higher, when the pressure p is set at p = 3 bar, see figure 7b.

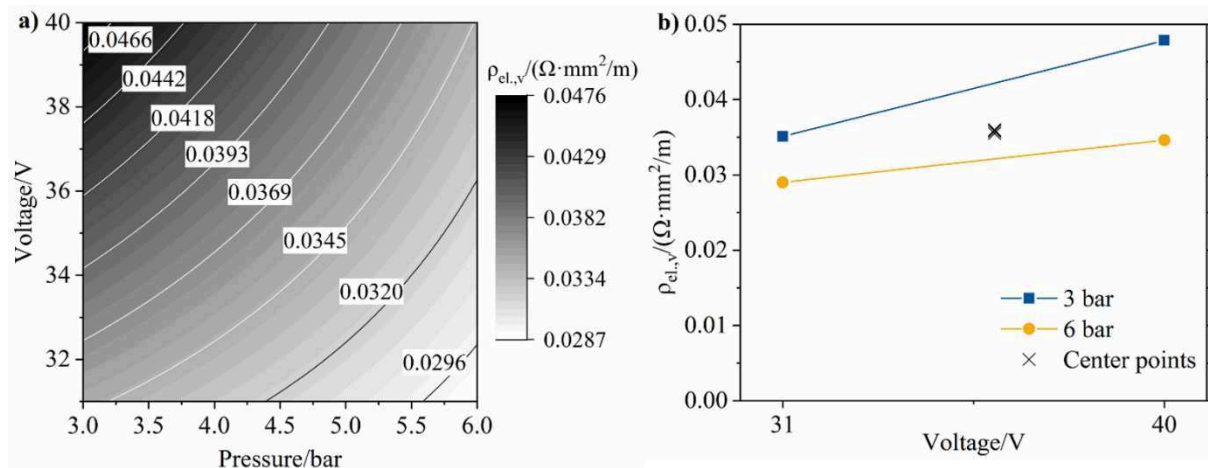


**Figure 7.** Contour plot of the correlation between  $\rho_v$ , the pressure and the voltage in case of Cu coating (a) and the interaction effect of the parameters (b).

### 3.3. Influence of the transfer process on the coating’s electrical resistance

Cu and Zn coatings were deposited with the parameter sets shown in Table 9. The two parameter sets have been determined as the best parameter sets for achieving low electrical resistivity of the coating in the characterization experiments for the two materials respectively.

**Table 9.** Process parameters used for the deposition of Zn and Cu coatings for the investigation of the influence of the transfer process on the coating’s electrical resistance.

Material	Wire diameter	Voltage	Feed rate	Atomizing gas	Gas pressure	Stand-off distance	Traverse velocity
<b>Zn</b>	1.6 mm	22 V	13.5 kg/h	N <sub>2</sub>	6 bar	50 mm	450 m/s
<b>Cu</b>	1.6 mm	31 V	10.5 kg/h	N <sub>2</sub>	6 bar	50 mm	675 m/s

The results shown in figure 8 confirms that there is no significant difference between the detached and transferred coatings regarding the electrical resistance. Therefore, it can be concluded that the transfer process has no considerable influence on the coating’s electrical resistance.

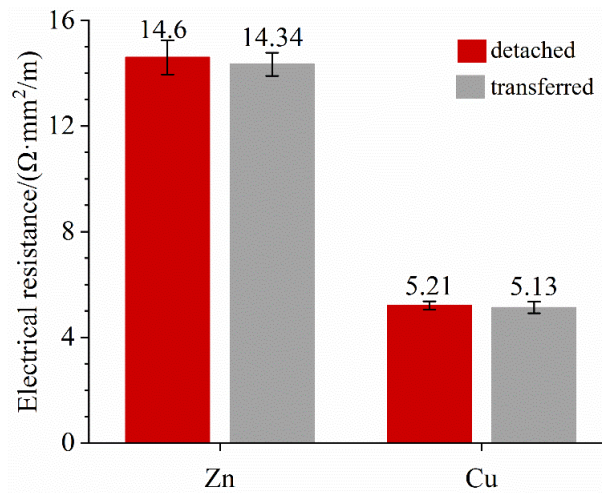


**Figure 8.** Comparison of the electrical resistance of the detached and transferred coatings.

#### 4. Conclusion

In case of Zn coatings, the stand-off distance shows the highest effect on the coating's electrical resistivity in the first stage of DoE. The wire diameter and the pressure show similar effects in this stage. To avoid the influence of the variation of the process condition on the investigation caused by changing the wires, only the stand-off and the pressure were included in the  $2^2$  full factorial design of experiment in the second stage of DoE. The effect of the wire diameter was investigated by a separate experiment series. The significance of the effects of the three parameters on the electrical resistivity of Zn coatings, which decreases with decreasing stand-off distance and wire diameter as well as increasing pressure, could be confirmed. Likewise, the stand-off distance shows the highest effect on the coating's electrical resistivity in the first stage of DoE for Cu coatings. However, the stand-off distance is not free adjustable for the aimed application. Therefore, the pressure and the voltage were investigated in the second stage. The decrease of the coating's electrical resistivity with increasing pressure and decreasing voltage could be confirmed.

The lowest electrical resistivity of the Zn and Cu coatings achieved in the current study was compared with the electrical resistivity of bulk Zn and Cu given in [24]. The electrical resistivity of the best Zn and Cu coatings was about 1.5 and 1.7 times that of the corresponding bulk materials, respectively, see figure 9.

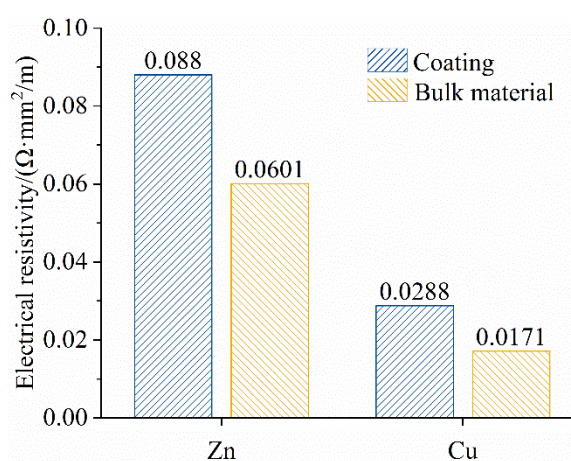


**Figure 9.** Comparison of the electrical resistivity of the coatings and the bulk material.

The influence of the transfer process on the coating's electrical resistance was investigated by the comparison of the electrical resistance of detached and transferred coatings. No noteworthy effect regarding this aspect could be determined in the investigation.

## 5. References

- [1] Huang W, Zhao Y, Fan X, Meng X, Wang Y, Cai X and Wang X 2013 *J. Therm. Spray Technol.* **22** 918–25
- [2] Liu A, Guo M, Zhao M and Hu M 2006 *Surf. Coat. Technol.* **200** 3073–7
- [3] Liu A, Guo M, Gao J and Zhao M 2006 *Surf. Coat. Technol.* **201** 2996–700
- [4] Ganesan A, Affi J, Yamada M and Fukumoto M 2012 *Surf. Coat. Technol.* **207** 262–9
- [5] Ganesan A, Yamada M and Fukumoto M 2013 *J. Therm. Spray Technol.* **22** 1275–82
- [6] Zhou X, Chen A, Liu J, Wu X and Zhang J 2011 *Surf. Coat. Technol.* **206** 132–6
- [7] Che H, Vo P and Yue S 2017 *Proc. Int. Thermal Spray Conf. (Düsseldorf)* (Düsseldorff/DVS Media GmbH) pp 98–103
- [8] Lupoi R and O'Neill W 2010 *Surf. Coat. Technol.* **205** 2167–73
- [9] Bobzin K, Hopmann C, Öte M, Linke T F, Liao X and Ochotta P 2017 Plastics-metal hybrid parts for electrical application *Integrative Production Technology - Theory and Applications* ed Brecher C and Özdemir D (Cham, Springer International Publishing) chapter 7 pp 519–44
- [10] Bobzin K, Öte M, Linke T F, Liao X, Hopmann C and Ochotta P 2015 *Therm. Spray Bull.* **67** 28–31
- [11] Hopmann C, Bobzin K, Schoeldgen R, Wunderle J, Linke T F and Ochotta P 2016 *J. Polym. Eng.* **36** 549–56
- [12] Bobzin K, Öte M, Knoch M A, Liao X, Hopmann C and Ochotta P 2016 *Proc. Int. Thermal Spray Conf. (Shanghai)* (Düsseldorff/DVS Media GmbH) pp 24–9
- [13] Bucci D 2017 Fundamentals of sensing and signal conditioning *Analog Electronics for Measuring Systems* ed Bucci D (London, John Wiley & Sons) chapter 1 p 30
- [14] Heaney M B 2004 Electrical conductivity and resistivity *Electrical Measurement, Signal Processing and Displays* ed Webster J G (Boca Raton, CRC Press) chapter 7 pp 7–4
- [15] Bobzin K, Öte M, Knoch M A, Liao X, Hopmann Ch and Ochotta P 2018 *J. Therm. Spray Technol.* **27** 119–34
- [16] Montgomery D C 2012 The 2<sup>k</sup> Factorial Design *Design and Analysis of Experiments* (Hoboken, John Wiley & Son) chapter 6 pp 233–303
- [17] Newberry A P, Grand P S and Neiser R A 2005 *Surf. Coat. Technol.* **195** 91–101
- [18] Szulc M, Zierhut J, Atzberger A, Schaup J, Hartz-Behrend K, Zimmermann S, Schein J, Krömmer W and Lang F 2016 *Proc. Int. Thermal Spray Conf. (Shanghai)* (Düsseldorff/DVS Media GmbH) pp 44–8
- [19] Oberg K E, Friedman L M, Boorstein W M and Rapp R A 1973 *Metall. Trans.* **4** 61–7
- [20] Sano K and Sakao H 1955 *J. Jap. Inst. Mater.* **19** 655–9
- [21] Gerlach J, Osterwald J and Stichel W 1968 *Z. Metallk.* **59** 576–9
- [22] Wilder T C 1966 *Trans. TMS-AIME* **236** 1035–40
- [23] Fischer W A and Ackermann W 1966 *Arch. Eisenhüttenw.* **37** 43–7
- [24] Haynes W M, Lide D R and Bruno T J 2017 Properties of Solids *CRC Handbook of Chemistry and Physics* (Boca Raton, CRC Press) chapter 12 pp 12–42–3

## Acknowledgments

The authors would like to thank the German Research Foundation DFG for the support of the depicted research within the Cluster of Excellence “Integrative Production Technology for High-Wage Countries”.